Geophysical Journal International

Geophys. J. Int. (2020) **223,** 471–487
Advance Access publication 2020 June 30
GJI Seismology

doi: 10.1093/gji/ggaa325

Detecting 1-D and 2-D ground resonances with a single-station approach

Giulia Sgattoni and Silvia Castellaro

Dipartimento di Fisica e Astronomia, Alma Mater Studiorum – Università di Bologna, viale Carlo Berti Pichat 8, 40127 *Bologna, Italy. E-mail: giulia.sgattoni@gmail.com*

Accepted 2020 June 26. Received 2020 June 7; in original form 2020 February 7

SUMMARY

The vibration modes of the ground have been described both in the 1-D and 2-D case. The 1-D resonance is found on geological structures whose aspect ratio is low, that is on layers with a lateral width much larger than their thickness. A typical example is that of a horizontal soft sediment layer overlying hard bedrock. In this case, the 1-D resonance frequency, traditionally detected by means of the microtremor H/V (horizontal to vertical spectral ratio) technique, depends on the bedrock depth and on the shear wave velocity of the resonating cover layer. The H/V technique is thus used both to map the resonance frequencies in seismic microzonation studies and for stratigraphic imaging. When 2-D resonance occurs, generally on deep and narrow valleys, the whole sedimentary infill vibrates at the same frequency and stratigraphic imaging can no longer be performed by means of the 1-D resonance equation. Understanding the 1-D or 2-D resonance nature of a site is therefore mandatory to avoid wrong stratigraphic and dynamic interpretations, which is in turn extremely relevant for seismic site response assessment. In this paper, we suggest a procedure to address this issue using single-station approaches, which are much more common compared to the multistation synchronized approach presented by research teams in earlier descriptions of the 2-D resonances. We apply the procedure to the Bolzano sedimentary basin in Northern Italy, which lies at the junction of three valleys, for which we observed respectively 1-D-only, 1-D and 2-D, and 2-D-only resonances. We conclude by proposing a workflow scheme to conduct experimental measurements and data analysis in order to assess the 1-D or 2-D resonance nature of a site using a single-station approach.

Key words: Seismic noise; Site effects; Geophysical methods.

1 INTRODUCTION

The vibration modes (or resonances) of the ground can be assessed by analysing its motion under microtremor excitation (Bard 1999; SESAME 2004; Haghshenas *et al.* 2008). However, seismic microtremor lacks a white spectrum and what we record on the Earth surface is modulated both by the seismic sources and the path travelled by the seismic waves. An efficient way to remove the source effect—that varies over time—and emphasize the path effect—that is characteristic of the site—was identified in the H/V ratio (horizontal to vertical spectral ratio, Nakamura 1989). This ratio has been shown to produce peaks in the H/V function at frequencies corresponding to the *SH*-resonance frequencies of the ground and is preferred, in the practical application, for its appearance that is much more stable in time—at any one site—compared to the individual spectral components.

At present, the H/V method is a widespread tool to map the resonance frequencies in seismic microzonation studies (Lermo and Chávez-García 1993, 1994; Lachet *et al.* 1996; Bour *et al.* 1998). The resonance frequency in the case of soils depends on their stiffness (quantified through the shear wave velocity, Vs) and on the thickness of the resonating layer. When an independent constraint on Vs is available, the resonance frequency can be translated into the depth of the local substratum, and *vice versa*. This has been used by several authors for stratigraphic imaging, both shallow (Parolai *et al.* 2002; Castellaro & Mulargia 2009a; Gosar & Lenart 2010; Mantovani *et al.* 2018) and deep (e.g. Ibs von Seht & Wohlenberg 1999; Zor *et al.* 2010; Sheib *et al.* 2016).

It has been shown over the years that an accurate interpretation of the H/V curve cannot ignore the observation of the individual spectral components (horizontals and vertical) used to produce it. This is essential to distinguish H/V peaks/troughs of stratigraphic origin from H/V peaks/troughs of anthropic origin (Castellaro & Mulargia 2010; Molnar *et al.* 2018). This is also essential to infer the nature of seismic waves involved in the observed resonance (body waves, laterally propagating surface waves, Castellaro 2016).

In a 1-D plane-parallel stratigraphic condition, the horizontal (e.g. NS and EW) spectral components must behave in the same way and we can assess that $\frac{NS}{V} = \frac{EW}{V} = \frac{H}{V}$, where H is normally meant as $H = \sqrt{\frac{NS^2+EW^2}{2}}$ (SESAME 2004).

However, when the geological layers can no more be interpreted as laterally infinite (2-D or 3-D conditions), for example in the presence of a sedimentary basin, then $\frac{NS}{V} \neq \frac{EW}{V} \neq \frac{H}{V}$. In this case, the spectra of the individual horizontal components (NS and EW) still contain information about the soil geometry and mechanical properties while this information becomes confused in the H/V ratio, where the individuality of the NS and EW components is mixed up. This is described in more detail in the following sections. In the worst scenario, the occurrence of 2-D phenomena is not acknowledged in the H/V data because erroneously interpreted as in the 1-D cases, ultimately leading to the wrong conclusions.

The 2-D resonance of sedimentary basins was studied theoretically (Bard & Bouchon 1980a,b; 1985; Chávez-García *et al.* 2000) and observed experimentally, mostly by means of synchronous recordings of ambient vibrations or by means of the reference site spectral ratio method (e.g. in the Rhône valley, Roten *et al.* 2006; Ermert *et al.* 2014; in the Grenoble basin, Guéguen *et al.* 2007; in the Romanche valley, Le Roux *et al.* 2012, in the Osaka sedimentary basin, Uebayashi *et al.* 2012).

Bard & Bouchon (1985) provided a function between the aspect ratio of a valley and the sediment-to-bedrock velocity contrast that should separate 1-D from 2-D resonance effects. In general, 2-D effects are expected in deep and narrow valleys.

Experimental studies on the valleys characterized by a 2-D dynamic behaviour report that steep sediment-bedrock interfaces and sharp lateral stratigraphic irregularities can lead to broad H/V peaks or flat H/V curves (e.g. Guillier *et al.* 2006). This is not unexpected by recalling that since $H = \sqrt{\frac{NS^2+EW^2}{2}}$, peaks occurring in the NS and EW components can both make the H/V peak appear larger as well as flattish.

Given the importance and the practical consequences of an appropriate identification of 1-D and 2-D resonance behaviours, in this paper we aim to suggest a procedure to face this issue by using single-station approaches. These are much more common in the daily practice compared to the synchronized multi-station approaches, that can often be practiced only by research centres.

We describe the procedure in a real case, that is the Bolzano sedimentary basin in Northern Italy, which lies at the junction of three valleys, for which we observed respectively 1-D-only, 1-D and 2-D, and 2-D-only resonances.

2 1-D AND 2-D RESONANCE OF THE GROUND

2.1 1-D resonance: theory and phenomenology

A number of theoretical studies showed that, in the case of horizontally 1-D layered geological structures, the H/V peak frequency is a good proxy to the *SH*-resonance frequency, f_0 (Lachet & Bard 1994; Lermo & Chavez-Garcia 1994; Fa¨h *et al.* 2001; Malischewsky & Scherbaum 2004; SESAME Project 2004; Haghshenas *et al.* 2008; Malischewsky *et al.* 2008; Lunedei & Albarello 2015). This is linked to the stiffness (quantified through the shear wave velocity, V_S) and the mass (quantified through the thickness h of the resonating layer, assumed to be infinitely extended in the horizontal directions):

$$f_n = (2n+1)\frac{V_S}{4h} \quad (1)$$

where $n = 0, 1, 2, \ldots$ is the natural vibration mode number.

Nakamura (1989, 2000, 2019) argued that the H/V peak frequency is caused by vertically incident *SH* waves, yielding a direct estimate of the *S*-wave transfer function and thus of site amplification. Numerical simulations (listed above) showed that the H/V peak frequency could also be due to the ellipticity of the fundamental Rayleigh waves, laterally propagating in the cover layers. The vertical component of Rayleigh waves contains no energy at the observed H/V peak frequency, being all Rayleigh waves linearly polarized on the horizontal component. This has been observed also in experimental studies (Castellaro 2016; Molnar *et al.* 2018).

Bonnefoy-Claudet *et al.* (2008) actually showed that the H/V peak frequency is a good proxy for the theoretical resonance frequency of vertically incident *SH* waves, both when microtremors are composed of body and/or surface waves. Later, Van del Baan (2009) showed that Love waves alone can be responsible for the observed resonance frequencies in sedimentary layers.

As noted in Castellaro (2016), the observation of the individual spectra used to produce the H/V curve at a site provides suggestions about the nature of the waves involved (Figs 1a and b). A local minimum at the resonance frequency in the vertical component may stand for the horizontal polarization of Rayleigh waves. Local maxima in the horizontal components may indicate a pure *SH* resonance or a dominance of Love waves.

In all cases, under a 1-D hypothesis, the horizontal spectral components coincide in the whole frequency domain and the H/V ratio settles down to amplitude 1 at any frequency far from the resonance ones. We recall that not all H/V peaks are of stratigraphic origin and the criteria to recognize them are given in Castellaro (2016).

Whatever the theoretical explanation behind the H/V, there is consensus on the fact that, when the 1-D assumption applies, spatial variations of the resonance frequency reflect changes in the sediment layer thickness, or a lateral variation of *Vs*. This led to several stratigraphic applications, such as the first bedrock mapping by Ibs von Seht & Wohlenberg (1999), followed by many other examples of bedrock and landslide mappings (references in the Introduction).

2.2 2-D resonance: theory and phenomenology

When the hypothesis of laterally infinite body vanishes, 2-D resonance applies. This generally occurs on geological structures whose dynamic behaviour is different along two main axes, due to a different geometrical (shape) or material stiffness in the two directions and shows up as two distinct (for frequency and amplitude) peaks in the horizontal displacement spectral components, acquired along the main axes (Figs 1b and d). The peak amplitude should be evaluated in the displacement spectra, because it is linked to the modal deformation.

In the 2-D case, the geological structure vibrates as a unique structure, with a transversal and longitudinal frequency of motion that depend on the object as a whole and do not vary in space. Reconstructing the geometry of the body is no longer possible by means of eq (1).

Bard and Bouchon (1980a,b, 1985) numerically studied this phenomenon on transversal sections of valleys, followed by other authors (Chavez-Garcia *et al.* 2000; Steimen *et al.* 2003; Frischknecht & Wagner 2004). They called the two emerging horizontal vibration modes, *SH* (out-of-plane motion, longitudinal to valley axis) and

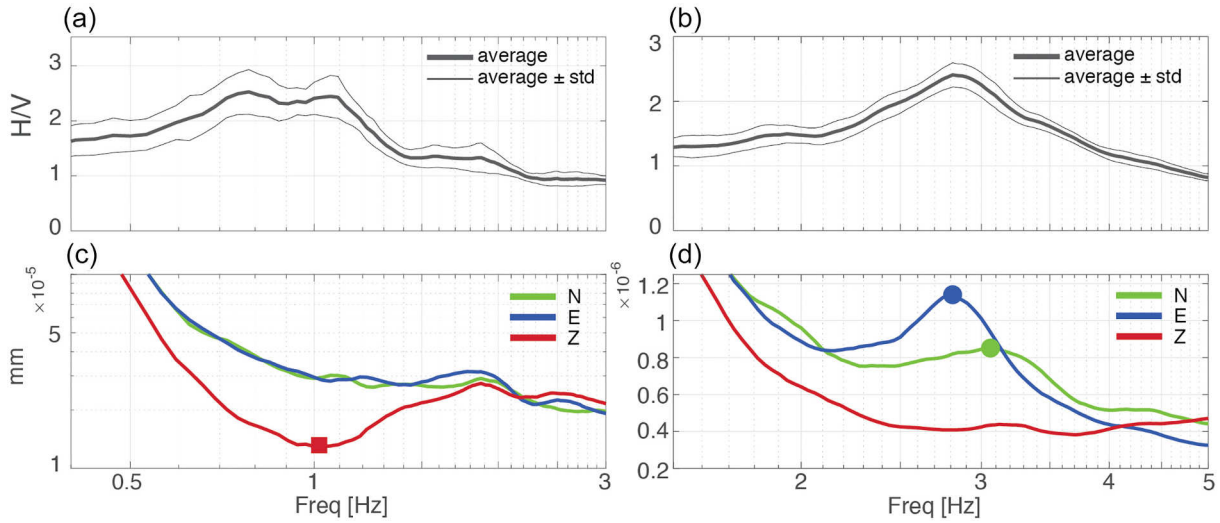

Figure 1. H/V curves (average ± standard deviation) obtained on (a) a 1-D stratigraphy (measurement site located in the Po plain near Bologna, Italy) and on (b) a 2-D stratigraphy (Arno river valley, Italy). In the 1-D case, the horizontal spectral components are overlapped and thus undistinguishable. (c) The H/V peak is generated by a local minimum in the vertical spectral component. In the 2-D case, the instrument was oriented with the E direction parallel to the valley axis. (d) The horizontal spectral components show two distinct peaks, at two different values and with different amplitudes, which reflect the different geometrical/shape stiffness of the sedimentary infill in the two directions.

SV (in-plane motion, transversal to valley axis), with $f_{SH} < f_{SV}$. While the *SH* mode is purely horizontal, the *SV* mode has a vertical component as well.

We note, however, that the natural vibration modes of an elastic body do not depend on the specific excitation and we therefore prefer to name them longitudinal (along the valley axis) and transversal (to the valley axis). We observe that $f_{LONG} < f_{TRAN}$, being the direction longitudinal to the valley axis the less stiff one for shape (we will assume that sediments are homogeneous in the two horizontal directions of the valley and therefore the material stiffness is homogenous as well). Consequently, this relation usually applies to the maximum displacement amplitudes: $A_{LONG} > A_{TRAN}$.

2-D modes are characterized by a constant frequency across the valley: what changes in space is the amplitude and phase, which depend on the mode shape.

Bard & Bouchon (1985) proposed some empirical equations to relate the 2-D frequencies (f_{LONG}, f_{TRAN}) to the width (w) and maximum depth of the valley (h_{max}) and to the theoretical 1-D frequency at the valley centre (f_c^{1D}):

$$f_{LONG} = f_c^{1D}\sqrt{1+\left(\frac{h_{max}}{w/2}\right)^2} \tag{2}$$

$$f_{TRAN} = f_c^{1D}\sqrt{1+\left(2.9\frac{h_{max}}{w}\right)^2} \tag{3}$$

For sine-shaped valleys, w is the valley half-width. Eqs (2) and (3) suggest that the deviation from the 1-D frequency increases with the aspect ratio (this was found also by Le Roux *et al.* 2012; and Cipta *et al.* 2018). However, for aspect ratios $\frac{h_{max}}{w} < 0.4$ the deviation of f_{LONG} (that is the most relevant amplification frequency) from f_c^{1D} is within 25 per cent, which is an acceptable value in applied geophysics.

Bard & Bouchon (1985) named critical shape ratio the h_{max}/w value above which 2-D resonance is expected. This value depends on the velocity contrast between sediment and bedrock. Later modelling by Moczo *et al.* (1996) suggested the existence of 2-D resonances also beyond the limits set by previous authors. The critical value should therefore be viewed as an approximate indication, also considering that equal h_{max}/w ratios apply to different valley shapes and possibly with heterogeneous filling sediments.

Here, we attempt to describe how to ascertain 2-D effects from the experimental data, not from the aspect ratio.

2.3 2-D resonance: sorting known principles into new hindsight

As already mentioned, what is called 2-D resonance in seismological applications is the resonance of any mechanical object, vibrating at the same eigenfrequencies at every location, with different amplitudes and phases. The traditional methods of mechanical and structural engineering can therefore be applied to derive some information about the geometry of the resonating body.

A first indication about the geometry of a homogeneous and isotropic resonating body is given by the ratio between its longitudinal and transversal modal frequencies. The closer they are, the lower the geometrical differences along the two axes.

As suggested by eq. (2) and (3), the ratio between the longitudinal and transversal eigenfrequencies $\frac{f_{LONG}}{f_{TRAN}}$, that can easily be measured on the field by means of single-station microtremor measurements, clears the dependence on the theoretical 1-D frequency at the valley centre (f_c^{1D}) and becomes a way to estimate the aspect ratio of the valley. This is illustrated in Fig. 2.

A second indication about the geometry of a resonating body comes from the sequence of its modal frequencies. This is known to depend on the slenderness.

In the case of a sine-shaped slab with the bottom edge fixed and a free surface (the top), that can be used as a simple prototype for a valley, the longitudinal (to the valley axis) modal frequencies are:

$$f_{mn} = f_c^{1D}\sqrt{(2m+1)^2+(n+1)^2\left(\frac{h}{w/2}\right)^2} \tag{4}$$

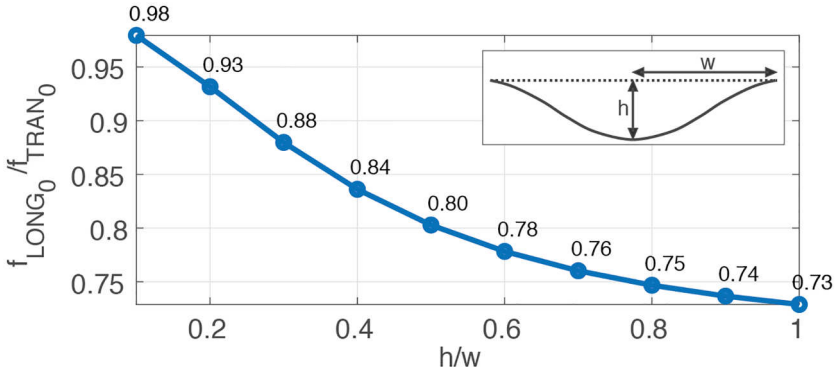

Figure 2. Ratio between the fundamental longitudinal (to the valley axes) f_{LONG} and transversal f_{TRAN} modal frequencies as a function of the aspect ratio of a sine-shaped valley, obtained by eqs (2) and (3).

Where $m = 0, 1, 2, \ldots$ is the order of the out-of-plane vertical mode and $n = 0, 1, 2, \ldots$ is the order of the horizonal longitudinal out-of-plane motion (Bard & Bouchon 1985, p. 535). We focus on the longitudinal modes because they exhibit the maximum amplitude and it is, in principle, easier to identify higher modes along this direction (blue curve in Fig. 1d). The ratio between the longitudinal out-of-plane modal frequencies (f_{00}, f_{10}, f_{20}, ...) is illustrated in Fig. 3. Again, this may be used to estimate the aspect ratio of the resonating structure.

3 EXPERIMENTAL OBSERVATION OF 1-D AND 2-D RESONANCES

We now describe the identification of 1-D and 2-D resonances in a real case and attempt a stratigraphic interpretation by exploiting the theoretical concepts provided in the previous sections.

3.1 The Bolzano sedimentary basin

The Bolzano sedimentary basin (Northern Italy) is characterized by a complex morphology because it lies at the junction between the 2–3 km wide Adige valley on the western and southern sides and two minor tributary valleys on the northern (Sarentino valley) and eastern (Isarco valley) sides (Fig. 4). Deep stratigraphic information is available from two seismic reflection profiles (SR1 and SR2 in Fig. 4, Pöyry 2017). These are about 2.5 km long and investigate a depth of around 1000 m. The SR1 profile across the Adige valley reveals reflectors outlining a U-shaped structure that reaches a maximum depth of about 700–900 m in the centre, and some horizontal reflectors down to 300 m depth. The SR2 profile reveals one main asymmetric reflector, reaching the maximum depth of 400 m at 1800 m distance from the northern end.

Direct deep stratigraphic information is available only about 20 km north west of the basin along the Adige valley, from a borehole located in the centre of the valley near the town of Sinigo. Here, the depth of the bedrock is constrained to 670 m (Bargossi *et al.* 2010). Another borehole in the town of Postal (15 km NW) detected the bedrock at 270 m depth.

The bedrock is made of porphyritic rock of Permian age while the basin fill is composed of fine- to coarse-grained quaternary deposits of fluvio-glacial to lacustrine origin.

3.2 Survey design

We collected single-station ambient noise recordings at 54 sites along three profiles, two of which located across the Adige valley (NS1 and EW1) and the third one located in the eastern part of the Bolzano basin (NS2; Fig. 4). All the recordings were acquired with two 3-D velocity microtremor recorders Tromino (MoHo srl, Italy) to make sure of the independence of the results from the specific instrument. They were collected during several field campaigns in winter, spring and summer 2019. Each measurement was acquired at 128 Hz sampling rate and lasted 14–16 min. Several measurements were repeated under different weather conditions and in different times of the year in order to verify their stability, for a total amount of 120 recordings. In particular, profile NS1 was surveyed twice in 2019 February and March, under sunny to partly cloudy weather conditions and four measurements in the central part were repeated also under heavy rain. Profile NS2 was surveyed in 2019 February under sunny weather and three measurements were repeated in 2019 July with cloudy to rainy conditions. Profile EW1 was surveyed in 2019 March under sunny conditions and several measurements on the edges of the profile were repeated in 2019 July and September with sunny to cloudy weather.

The instruments were oriented with their axes parallel to the longitudinal and transversal morphological axes of the basin at each site. Orienting the instrumental axes along the structural axes is mandatory, in order to interpret the results. The common recommendation, found in many guidelines of microtremor acquisition, of orienting the instruments along the NS–EW direction is not relevant in the 1-D case (where the response is the same in all the horizontal directions) but is definitely not to be followed in the 2-D case. Exactly as in the structural (building, bridges, etc.) dynamic studies, instruments should be placed with the axes parallel to the structure in order to assess the dynamic behaviour around those axes. Failing to do so has the consequences described in Section 7.

We also acquired ambient noise simultaneously at five sites along the NS1 section (Fig. 4) in order to study the modal shapes. The simultaneous acquisition was performed by exploiting the instrumental built-in radio transmission/reception modules, that ensure a clock and sampling rate correction every second, and lasted 20 min.

3.3 Data processing

Each waveform was split into 30 s non-overlapping windows, detrended, tapered with a Bartlett window, padded, FFT-transformed

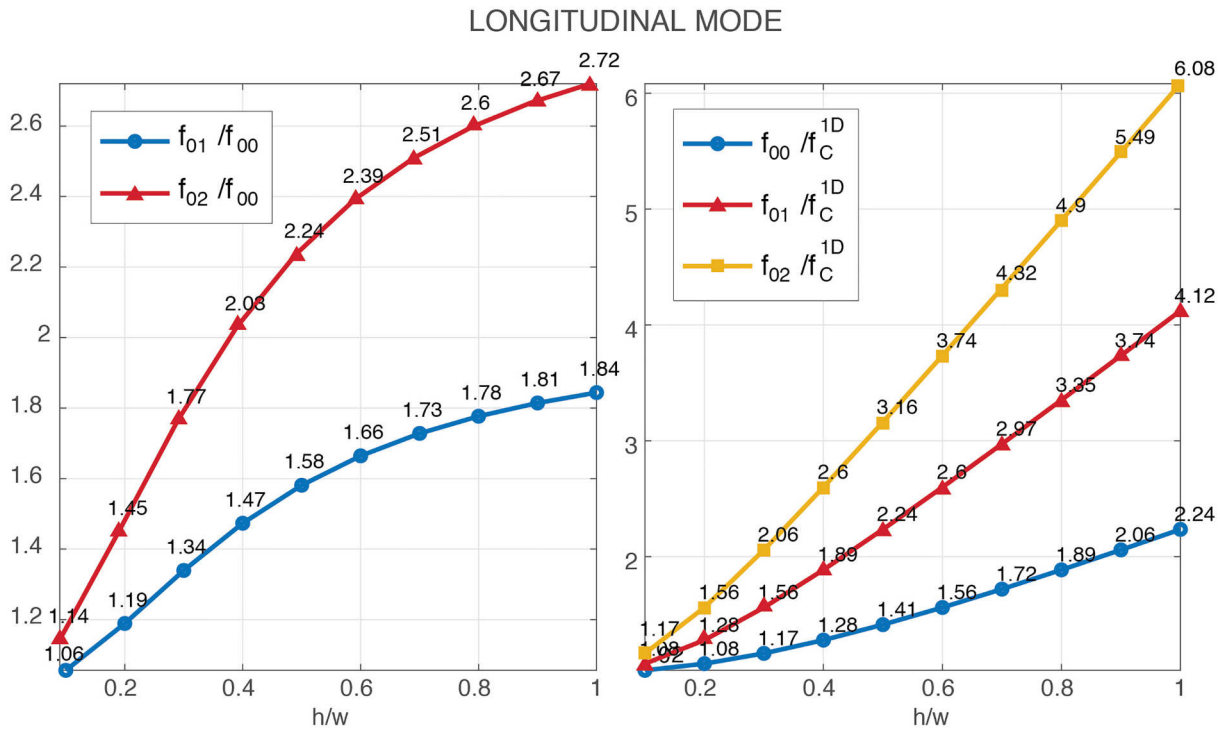

Figure 3. Ratios between longitudinal (to the valley axis) modal frequencies, obtained by using eq (4). Left: dimensionless ratio between the second and the first modal frequencies ($\frac{f_{01}}{f_{00}}$, blue curve) and the third and first modal frequencies ($\frac{f_{02}}{f_{00}}$, orange curve), as a function of the aspect ratio. Right: same as left, but compared to the theoretical 1-D frequency at the valley centre f_c^{1D}.

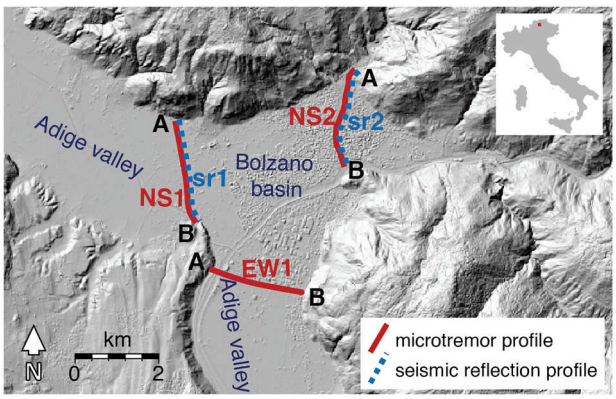

Figure 4. Location of the Bolzano basin in Italy. SR are the seismic reflection lines, NS1, NS2, and EW1 are the sections along which ambient noise recordings were acquired.

and smoothed with triangular functions having a width equal to 10 per cent of the central frequency.

Care was taken in the removal of transient disturbances from the curves, by operating a manual selection.

Both the individual component spectra and the H/V ratios were computed (in terms of average ± standard deviation) for each site.

According to the basic rules of spectral analysis, a 30 s signal allows for a good spectral reconstruction down to 0.13 Hz (corresponding to one-fourth of the signal length). In order to be sure that results are not affected by the processing parameters, a few longer (40 min) recordings were analysed by splitting them into longer windows (up to 60–80 s) but results did not change.

4 OBSERVATION OF 1-D AND 2-D VIBRATION MODES ON THE INDIVIDUAL SPECTRAL COMPONENTS

4.1 Modal frequencies

Because we are interested in the deep sediment-to-bedrock interface and in its effects on the dynamic behaviour of the valley, we focus on the fundamental (the lowest) H/V peak frequencies and on the corresponding features of the individual spectral components.

As recalled in Section 2, the 1-D resonance is marked by a trough in the vertical spectral components, while the 2-D resonance is marked by peaks in the horizontal spectral components, typically occurring at different frequencies. In the Bolzano basin, we met both these features (Fig. 5).

The local minimum at the lowest possible frequency in the vertical component is marked with a red square in Fig. 5(b): this is interpreted as a common 1-D resonance. The horizontal spectral peaks corresponding to the longitudinal and transversal modal frequencies are marked with blue and green circles in Figs 5(a) and (c). These are interpreted as 2-D resonances.

We performed the picking of the local minima of the vertical component and of the local maxima of the horizontal ones on all the recordings acquired along the NS1, NS2 and EW1 profiles (Fig. 6).

An overview of Fig. 6 (top panel) suggests that the dynamic behaviour of the Bolzano basin along the NS2 section is definitely 1-D. The longitudinal and transversal horizontal spectra do not differ in the whole frequency domain, while the vertical spectra show a local minimum, the frequency of which changes along the section from 0.4 to 9 Hz, following the buried valley geometry (that is moving from low to high frequencies, as the bedrock becomes shallower).

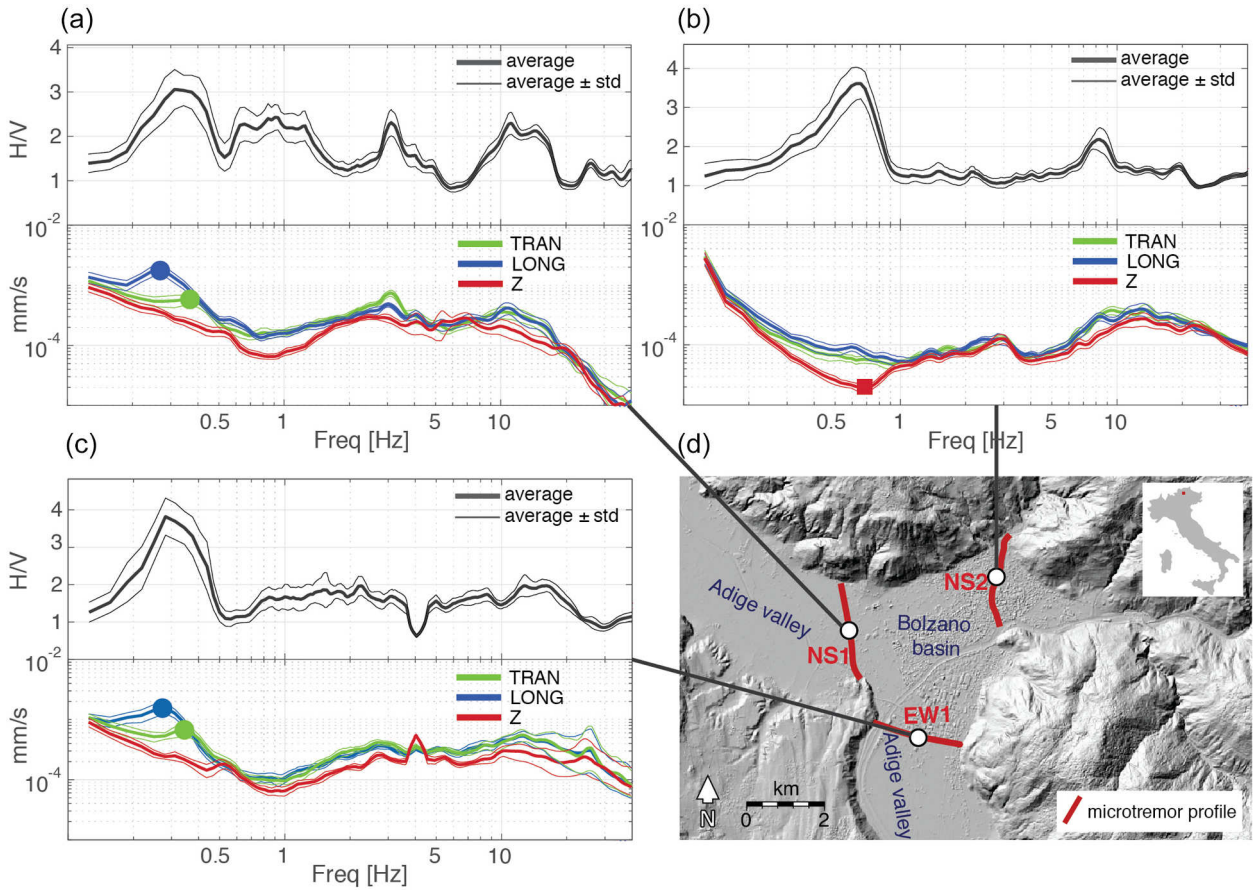

Figure 5. (a)–(c) examples of single-station ambient noise measurements recorded on the surveyed profiles (top: H/V ratio and bottom: individual spectral components of motion). For each H/V curve and individual component spectrum the relative confidence interval is given. The latter is anyway smaller than the former (Castellaro & Mulargia 2009b). In (a) and (c), the green and blue circles mark the longitudinal and transversal 2-D resonance peaks. In (b), the red square marks the local minimum of the vertical component at the 1-D resonance frequency. (d) Map of the study area (Digital Surface Model from Geoportale Alto Adige).

The dynamic behaviour of the southern branch of the Adige valley (Fig. 6, bottom panel) is, on the opposite, 2-D. Here, the horizontal spectral components show a peak at 0.28 $\pm$ 0.02 Hz in the direction longitudinal to the valley axis and a peak at 0.33 $\pm$ 0.03 Hz in the direction transversal to the valley axis. The frequencies are significantly different, clearly marking the different geometrical stiffness in the two directions (the mechanical properties of the filling sediments being approximately the same in the two directions) but the whole valley vibrates at these same frequencies. The reconstruction of its geometry can thus no longer be performed by using eq. (1).

The dynamic behaviour of the western branch of the Adige valley (Fig. 6, central panel) is 1-D on the sides and 2-D in the central part. On the sides, the frequency shift of the vertical spectral minima suggests that there is a local control on the resonance. In the central part we observe a clear horizontal longitudinal spectral peak (0.28 $\pm$ 0.02 Hz) and a clear horizontal transversal peak (0.36 $\pm$ 0.03 Hz), occurring at the same frequency at different sites. This stands for the fact that the central part of the valley behaves as a unique body from a dynamic point of view while laterally propagating surface waves dominate on the edges. The 2-D spectral peaks become naturally less visible while approaching the valley edges, which are the nodes with zero displacement (see also Section 4.2). For this reason, we did not mark them with circles in Fig. 6. However, it should be noted that these peaks appear lower than real due to the use of a logarithmic amplitude scale, which was necessary to improve the visibility of the spectra in the whole frequency range.

We note again that, in all the 2-D cases, the longitudinal-to-the valley spectral peak has always a larger amplitude compared to the transversal-to-the valley spectral peak. This is a natural consequence of the geometry of the valley and of its directional stiffness properties. This amplitude difference can well be observed in the velocity spectra S_v of Fig. 6 (central and bottom panels) and would be even more visible if the same spectra were plot in displacement S_d, being $S_d = \frac{S_v}{2\pi f}$ and being $f_{\mathrm{TRAN}} > f_{\mathrm{LONG}}$. We decided to plot the spectra in terms of velocity, because the data were recorded in terms of velocity, being acquired by seismometers.

4.2 Modal shapes

In order to visualize the modal shapes, we performed simultaneous noise measurements at five sites along the lower half of NS1 section (Fig. 4). The results were mirrored around the central axis to cover also the upper half of the section, assuming symmetry of the valley. Acquiring simultaneous measurements is not mandatory to pick the modal frequencies but it helps in assessing modal shapes and is here presented to support the findings described in Section 4.1. The microtremor signal was converted to displacement, then filtered at the frequency of the first longitudinal mode (0.28 Hz).

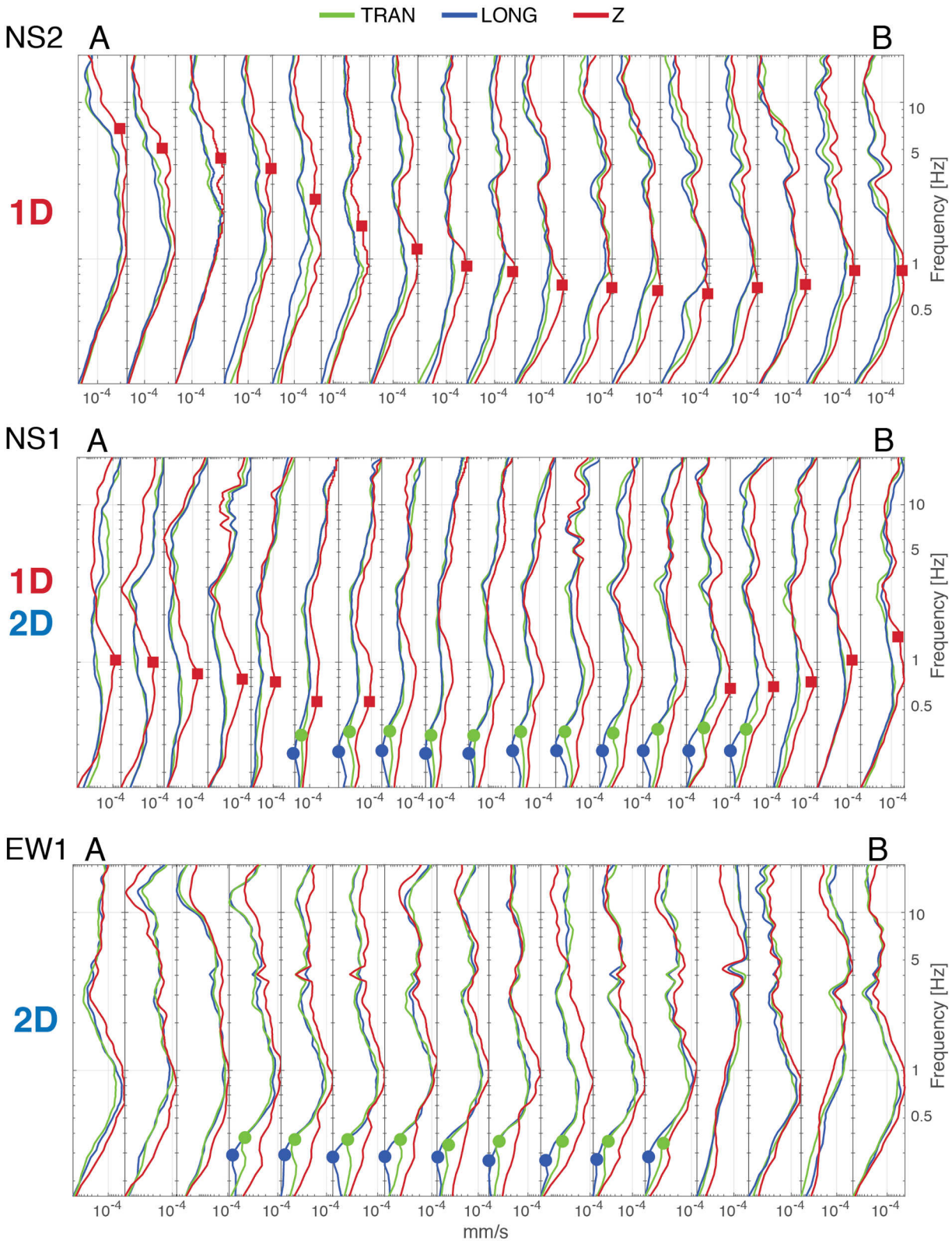

Figure 6. Individual spectral components of motion of all measurements acquired along the three profiles of Fig. 4. The blue circles mark the horizontal longitudinal fundamental mode frequency, f_{LONG}. The green circles mark the horizontal transversal fundamental mode frequency f_{TRAN}, for the sites where 2-D resonance is recognized. The red squares mark the minimum in the vertical spectral component that indicates 1-D resonance. The spatial variation of the 1-D resonance frequencies is clear, compared to the stability of the 2-D resonance frequencies.

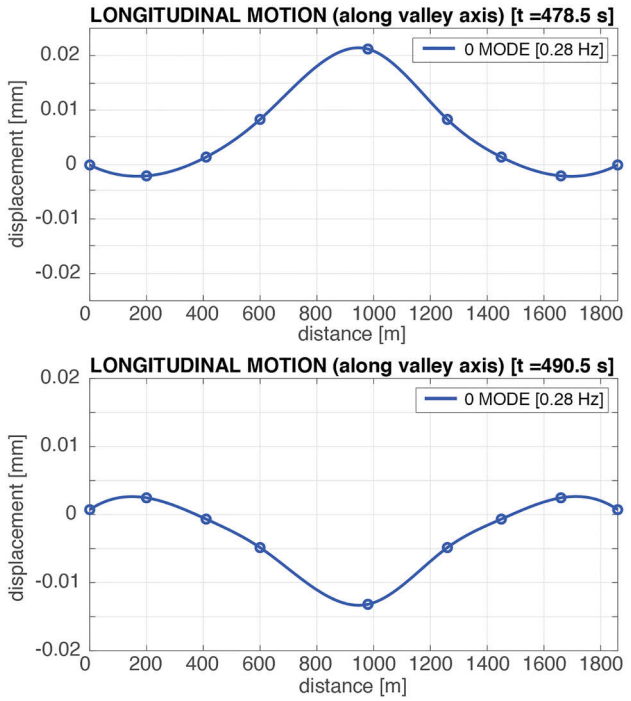

Figure 7. Mode shape of the fundamental longitudinal mode of the valley, at the NS1 section, along its longitudinal axis.

The resulting modal shape is illustrated in Fig. 7 for two instants of time and is that of the fundamental longitudinal mode, thus having no points of zero displacement beyond the two ends, that are fixed.

It is very interesting to observe that the real displacement does not start at the valley edges but at about 500 m distance from them, that is at about one-fifth of the valley width. This can reflect on one side the nature of the constraint: in structural terms, this would be the behaviour of a body fixedly jointed on the side edges. On the other side, this might also explain (or be a consequence of) the fact that on this valley a 1-D resonance behaviour is observed at the edges (red squares in Fig. 6) and the 2-D resonance behaviour is observed in the central part.

5 OBSERVATION OF 1-D AND 2-D VIBRATION MODES ON THE H/V CURVES

We now move to the description of the phenomenology of the H/V curves acquired on a sedimentary basin showing 1-D and 2-D dynamic behaviours.

5.1 Spatial distribution of the H/V peak frequencies

Both the spectral patterns described for the 1-D and 2-D resonance produce peaks in the H/V ratios. Although the shape of a single H/V peak alone cannot be used to discern between 1-D or 2-D resonance, the spatial variation of resonance frequencies depends (also) on the resonance type.

Fig. 8 illustrates the H/V curves arranged along the surveyed cross-sections in the Bolzano basin. The H/V peaks associated to the bedrock are connected by a dashed line. All profiles show the H/V peak frequencies decaying towards the centre, but with different patterns in terms of spatial variation of frequency.

In the 1-D section (NS2 profile in Fig. 4), where eq. (1) applies, the H/V peak frequency, shifting from 0.5 to 9 Hz, follows the geometry of the buried valley (Fig. 8, top). This is due to the shift of the minimum in the vertical spectra component seen in Fig. 6, while the longitudinal and transversal horizontal spectra do not differ in the whole frequency domain.

In the 2-D section (EW1 profile in Fig. 4), the H/V frequency remains constant (Fig. 8, bottom), as were the peaks in the horizontal spectral components described earlier (Fig. 6). This implies that the central part of the valley resonates as a single body and the H/V peak frequency cannot straightforwardly map the bedrock depth at each location. A less clear variation of the H/V frequency peaks can be observed on the valley edges.

In the 1-D + 2-D section (NS1 profile in Fig. 4), a clear shift of the H/V frequency at the valley edges and a stabilization of the H/V peak frequency in the central part are observed (Fig. 8, centre). The dashed lines in Fig. 8 connect the main H/V peaks that are associated to 1-D resonance (that is due to local minima in the vertical spectral component) on the profile edges and 2-D resonance in the central part of the profile (due to local maxima in the two horizontal components; Fig. 6). Low amplitude peaks associated to 2-D resonance may still be observed in the H/V curves also towards the edges of the valley. Their amplitude is smaller because the fundamental mode shapes (Fig. 7) approach the nodes (zero displacement positions). The H/V curves shown in Fig. 8 are individually normalized and therefore very high peaks hamper low ones. The reader may refer to Fig. 9 for an easier quantification of spectral ratio amplitudes.

5.2 H/V, transversal/V and longitudinal/V amplitudes

As we recalled, the amplitude of the individual spectral components of microtremor measurements acquired at different sites and at different times can be used to reconstruct modal shape, provided that the excitation level is stationary at all sites. Alternatively, synchronous measurements are needed. However, since the H/V function has the power to clear source effects (see the Introduction, Nakamura 1989; Castellaro 2016), the amplitude variation of the H/V (even of those recorded at different times) over space can still have some meaning.

Because a 2-D resonance has different effects on the horizontal components, we analysed the peak amplitude pattern in terms of H/V, transversal/V and longitudinal/V along the three surveyed sections (Fig. 9). The amplitudes were evaluated at the 1-D resonance frequencies along profile NS2 and at the 2-D resonance frequencies along profiles NS1 and EW1. We recall that along profile NS1 we observe both 1-D and 2-D resonance phenomena, however we choose here to investigate the amplitude behaviour of the 2-D resonance mode and therefore evaluate spectral amplitudes at the 2-D resonance frequency along the whole profile. The data along each profile were acquired in different days and/or weather conditions, but were all processed with the same criteria (i.e. same window length, same smoothing, etc.) in order to make the results comparable. The peak amplitudes of recordings performed on the same day are connected by a line. The symbols not connected by lines

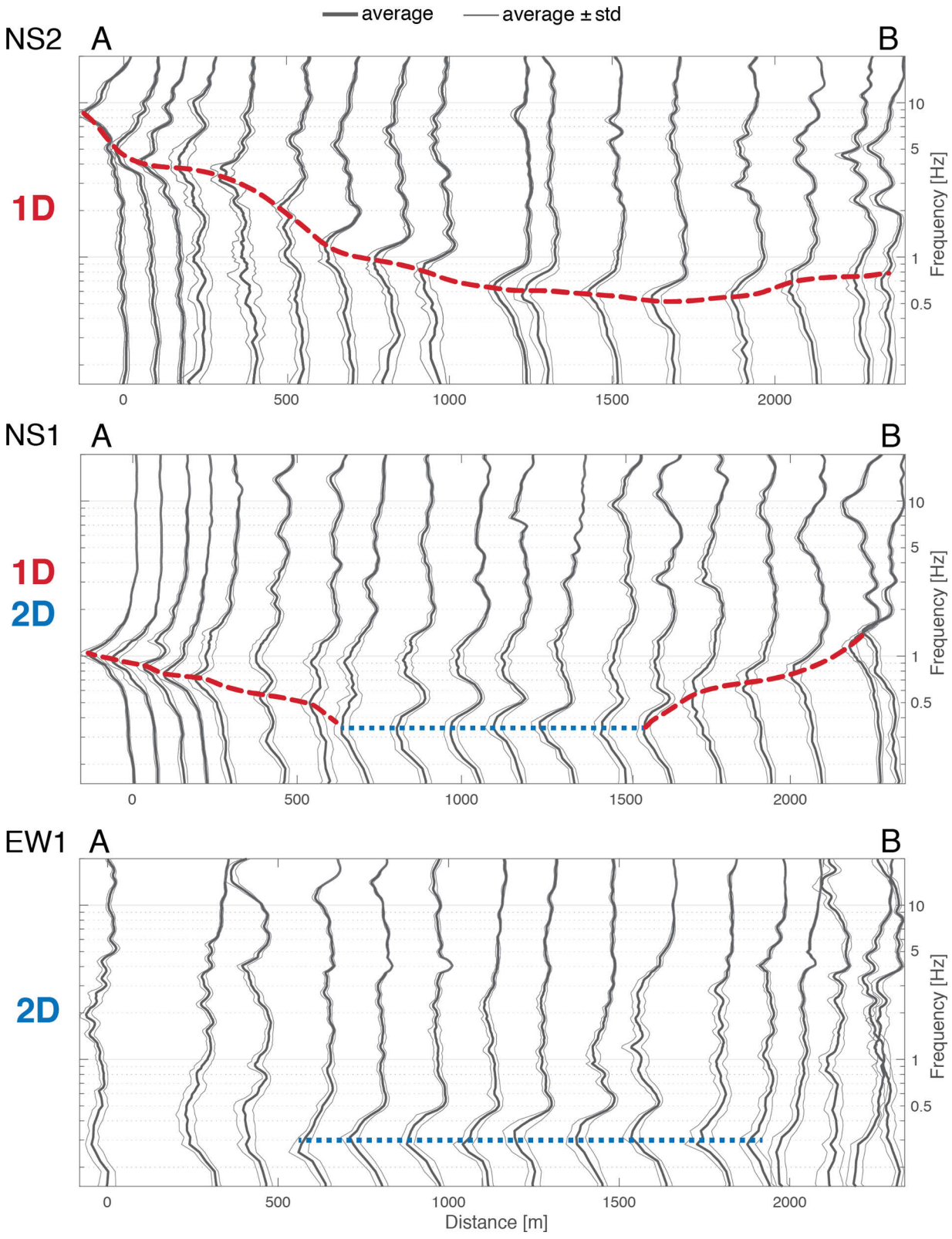

Figure 8. H/V curves at different sites along the three investigated profiles (Fig. 4). The blue dashed lines mark the H/V peak frequencies that do not vary in space (2-D resonance). The red dashed lines mark the H/V peaks with frequency varying over space (1-D resonance).

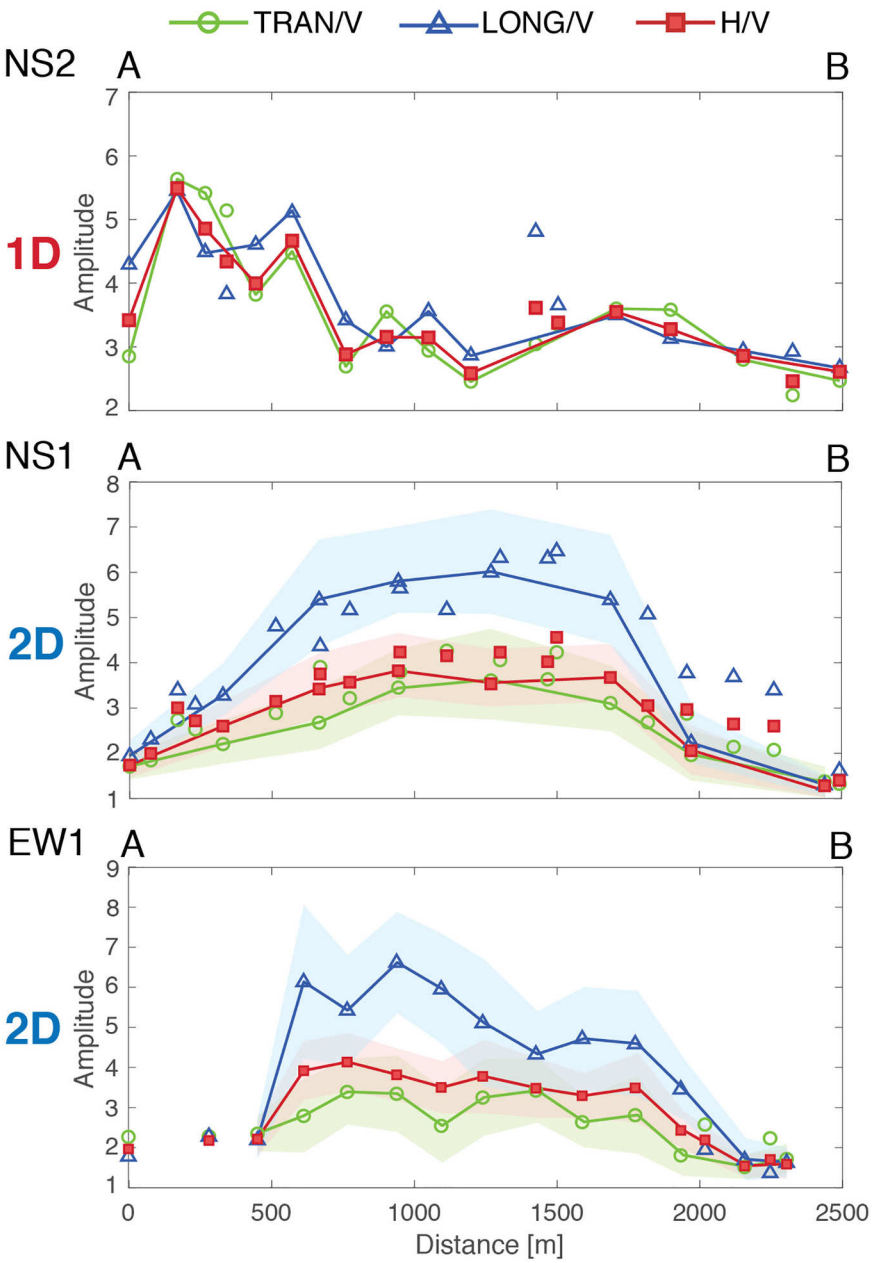

Figure 9. H/V, transversal/V and longitudinal/V peak amplitude along the surveyed sections evaluated at the 1-D resonance frequencies along profile NS2 and at the 2-D resonance frequencies for profiles NS1 and EW1. The shaded areas on the 2-D profiles represent the confidence intervals. These are not drawn on the 1-D profile not to impair readability, but are of the same order of magnitude as for the other profiles.

refer to peak amplitudes acquired on different days. It can be observed that a mild dependence on seasons and weather conditions still exists. However, this does not prevent us from observing a clear pattern:

(i) In the 1-D case (Fig. 9, top panel) the transversal/V and longitudinal/V ratios coincide, and so does the H/V ratio. Since the H/V peak frequency depends on the local bedrock depth, its amplitude should reflect the local impedance contrast. On average, this is expected to be higher at the valley edges, where the sediments are shallower and less compacted by gravitation and lower at the valley centre. This clearly applies only if the sediments are the same in the whole basin.

(ii) In the 2-D cases (Fig. 9, central and bottom panel), the transversal/V and longitudinal/V peak amplitude should reflect the respective mode shapes, and therefore be larger at the centre and tending to zero at the edges for the first eigenmode of the valley. This clearly applies provided that the vertical ratio does not present peaks/troughs *per se* at some sites. Although the features of 2-D resonance should be looked for in the individual horizontal components, the effect on the H/V function can also be interesting. Since the H/V ratio represents an average of the horizontal components, the H/V peak amplitudes, as expected, have a similar trend and intermediate amplitudes between the transversal/V and longitudinal/V.

(iii) As expected (Section 2.2), the longitudinal/V peak amplitude is always larger compared to the transversal/V peak amplitude.

Ermert *et al.* (2014) observed that the 2-D modal shapes reflect the bedrock shape. This is true for the fundamental longitudinal vibration mode and can be explained thinking that the free length of inflection of the sedimentary cover increases as the bedrock becomes deeper. The longitudinal/V amplitude patterns therefore might suggest that the sediment-to-bedrock interface across the Adige valley is symmetric in the western valley (NS1) and asymmetric in the southern valley (EW1).

6 FREQUENCY TO DEPTH CONVERSION

6.1 In the 1-D case

Now that the vibrational modes of the Bolzano basin have been assessed, it is interesting to attempt a stratigraphic reconstruction.

We start from the NS2 profile (Fig. 4), dominated by 1-D resonance, where the H/V frequency can be translated into depth information. This requires a V_S model, that can be reconstructed when the depth of a layer causing resonance in the H/V curve is known (Castellaro & Mulargia 2009a). In the case of multiple H/V curves acquired along alignments, if spatial homogeneity of the sedimentary cover can be assumed and gravity compaction is the only factor causing a gradual increase of V_S with depth, a power-law regression model can be derived by fitting resonance frequencies with known depths of the resonating layer (Ibs-von Seht & Wohlenberg 1999).

We used this approach, by constraining the H/V inversion with the information from the seismic reflection profiles (Pöyry 2017). We used the seismic reflection profile SR2 acquired within the Bolzano basin, which fixes the maximum bedrock depth to 400 m. We associated this depth to the H/V peak frequency collected at the centre of the NS2 section (Fig. 4), that is 0.5 Hz. We used other 15 points picked from the seismic reflection profile and correlated them to the corresponding H/V peak frequencies, thus obtaining the frequency–depth relation of Fig. 10. In the end, this model was used to convert the H/V curves from the frequency to the depth domain at all the 1-D sites, thus imaging the bedrock morphology. These H/V-depth curves acquired at each site along the NS2 profile are plotted in Fig. 11, where H/V peaks are indicated in shades of red. These are overlaid with the seismic reflection profile and show the correlation between the two techniques.

6.2 In the 2-D case

We now focus on the NS1 section, because a seismic reflection profile is available for crosscheck there as well. As already described, along this section 1-D resonance can be observed at the two valley edges (for about 500 m on each side). Here, the H/V can be used as a stratigraphic tool, as done in the previous section and this leads to the H/V contour plot of Fig. 12, that matches the reflection seismic.

Reconstructing the valley morphology in the central part, where 2-D resonances are detected, is more problematic because the measured resonance frequencies do not vary with space. This is apparent in the central part of Fig. 12, where the H/V curve has peaks stabilized around the same value. We will therefore apply the criteria illustrated in Section 2.3.

We note that, as described in Section 4.1, $\frac{f_{\mathrm{LONG}}}{f_{\mathrm{TRAN}}} = \frac{0.28\ \mathrm{Hz}}{0.36\ \mathrm{Hz}} = 0.78$ and this stands, according to Fig. 2, for an aspect ratio of 0.6. Given that in the inspected section $w \simeq$ 1000–1200 m, this suggests that the maximum valley depth is $h_{\max} \simeq$ 600–700 m.

This is possibly confirmed by direct stratigraphic information from a borehole located in Sinigo, about 20 km north west of Bolzano, where the Adige valley is 670 m deep (Bargossi *et al.* 2010).

We note, however, that in this case, characterized by low frequency values, slight uncertainties in the natural frequencies lead to variations in the $\frac{f_{\mathrm{LONG}}}{f_{\mathrm{TRAN}}}$ ratios that turn into large variations in the estimated aspect ratios (Figs 2 and 3). These methods can therefore be used only as rough approximations.

In the case of higher frequency values, where uncertainties are usually lower, the estimate of the aspect ratio would be less affected. Thus, when dealing with deep valleys, errors in the reconstruction of the bedrock depth are intrinsically larger. However, this applies to any geophysical technique.

About the 2-D, EW1 profile, we observe that the longitudinal and transversal frequencies experimentally measured are similar to those discussed for the NS1 profile. Since the two valleys have comparable widths, this suggests they have also a similar maximum depth, the origin of the two valleys being the same.

More problematic is how to reconstruct the bedrock geometry, since the 2-D laterally constant frequencies cannot be linked to the laterally changing geometry of the sediment-bedrock interface. As mentioned in Section 5.2, some hints can be obtained from the longitudinal/V amplitude pattern of the 2-D resonance peaks across the valley, which can be used as a proxy to the 2-D fundamental longitudinal mode shape. In the EW1 profile, we note an asymmetric pattern (Fig. 9), which suggests an asymmetric geometry of the sediment-bedrock interface with the maximum sediment thickness expected at around 600–1100 m distance from the western end.

7 DISCUSSION AND CONCLUSIONS

In this paper, we reviewed and sorted the theoretical and phenomenological aspects of 1-D and 2-D resonances of geological structures and described new elements that can allow for a better discrimination between the two dynamic patterns. Understanding the 1-D or 2-D resonance behaviour of a site is mandatory both for seismic site effects assessment as well as for stratigraphic reconstructions. Failing to do so, leads to wrong conclusions in both cases. We focused on the single-station approach, which is much more common in the daily practice compared to the multistation synchronized approach presented by research teams in the earlier description of the 2-D resonances. While multistation measurements are needed for any phase analysis, the single-station approach can still be sufficient to detect the fundamental 2-D resonance frequencies and discern between the 1-D versus 2-D resonance behaviour of a site. A peak in the H/V function can be associated to either a local minimum in the vertical spectral components and/or local maxima in the horizontal components. Because the footprints of 1-D versus 2-D resonance phenomena reside in the shape of the individual spectral components, the H/V ratio has to be analysed always in conjunction with the individual spectra of motion in order to distinguish between the two dynamic behaviours and to identify the 2-D resonance frequencies.

The so-called 1-D resonance is found on geological structures whose aspect ratio $\frac{h}{w}$ is low, that is on layers with a lateral width much larger than their thickness. It has been shown that whatever the origin (resonance of body waves, lateral propagation of Rayleigh or Love waves, see Section 2.1), this type of resonance changes

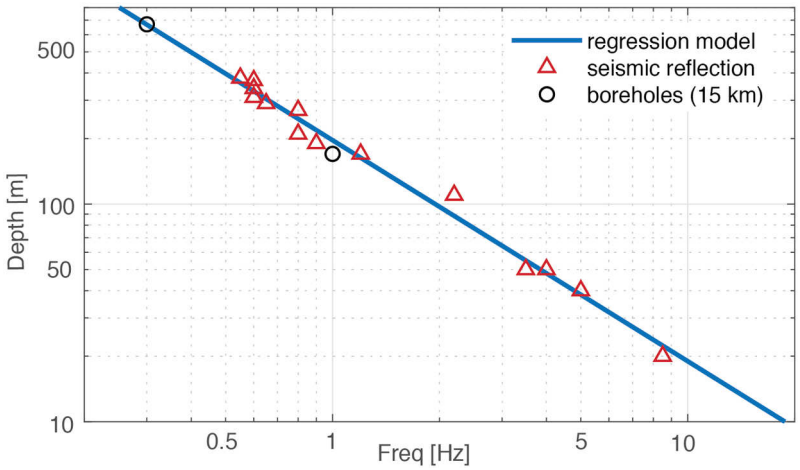

Figure 10. Resonance frequencies and corresponding depth to bedrock estimated from the seismic reflection survey at 16 control sites. The location of each site is indicated by the arrows at the bottom of Fig. 11. The data are fitted to a power-law model, represented by the blue line. The circles correspond to two boreholes located 15 km NW of section NS1 along the Adige valley.

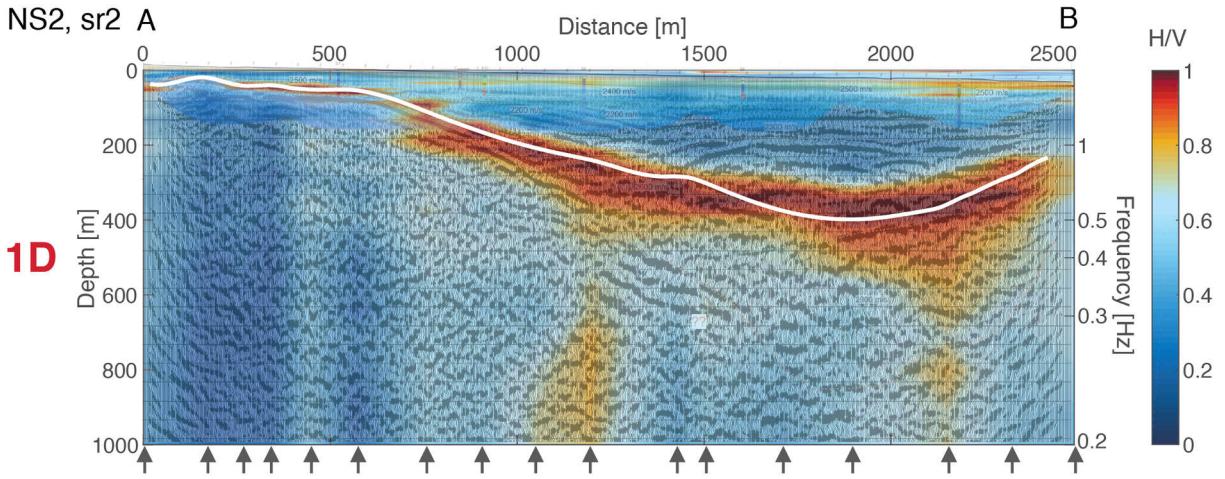

Figure 11. H/V contour plot of the NS2 profile, overlaid with the seismic reflection profile (Pöyry 2017). The white line indicates the position of the sediment-bedrock interface inferred from seismic reflection and used to constrain the H/V model. The arrows indicate the positions of the single H/V curves. Each H/V curve was normalized so that the colour scale ranges from 0 (blue) to 1 (red).

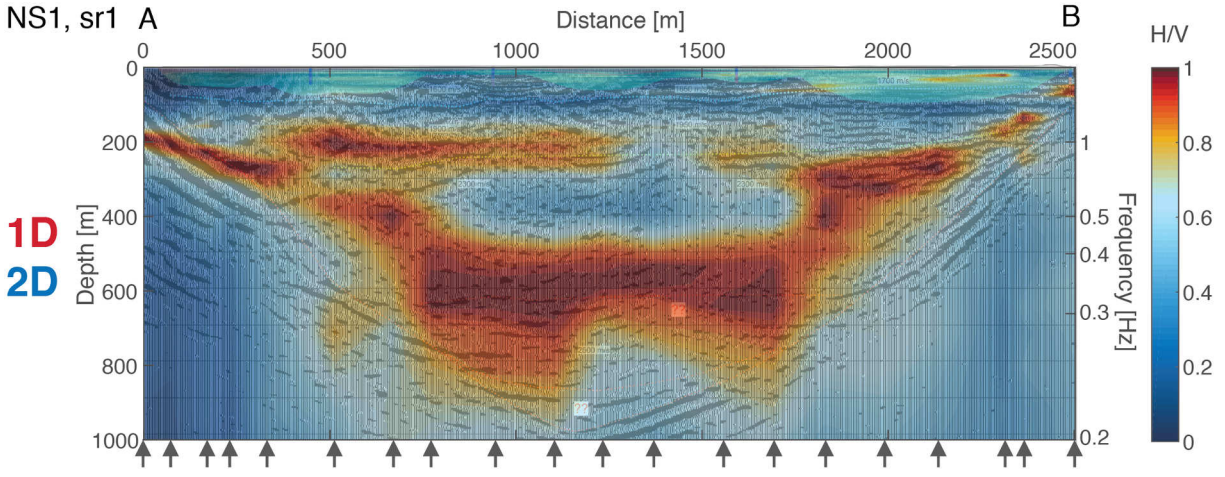

Figure 12. H/V contour plot of the EW1 profile, overlaid with the seismic reflection profile (Pöyry 2017). The arrows indicate the positions of the single H/V curves. Each H/V curve was normalized so that the colour scale ranges from 0 (blue) to 1 (red).

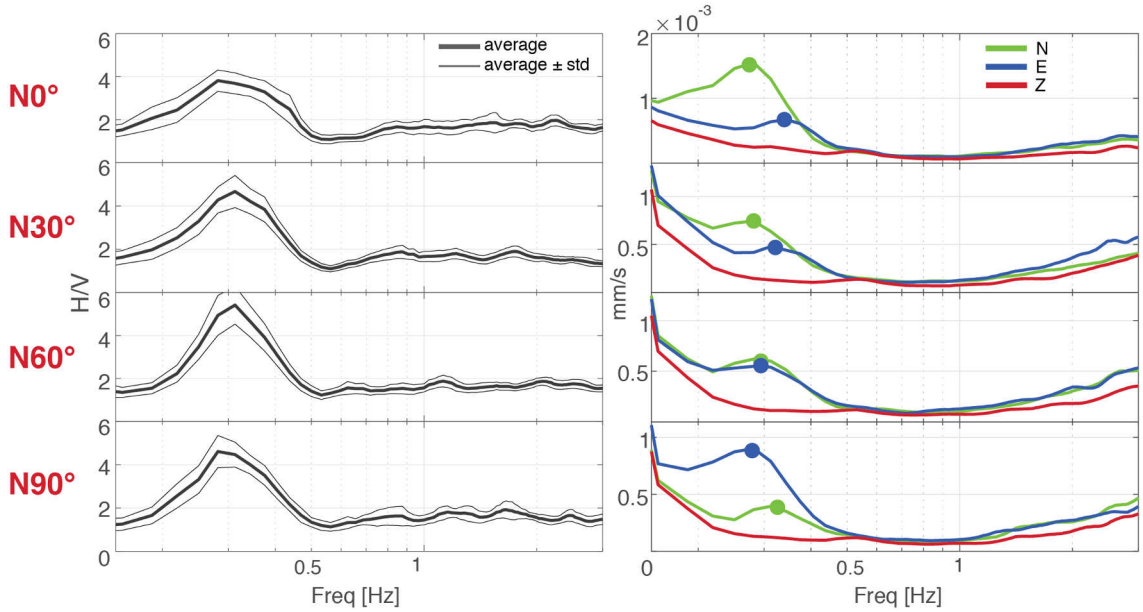

Figure 13. H/V measurements acquired with different instrument orientation. From top to bottom: instrumental north parallel to the valley axis and with a clockwise rotation of 30°, 60° and 90° with respect to the valley axis. The green and blue circles mark the resonance peaks on the horizontal components.

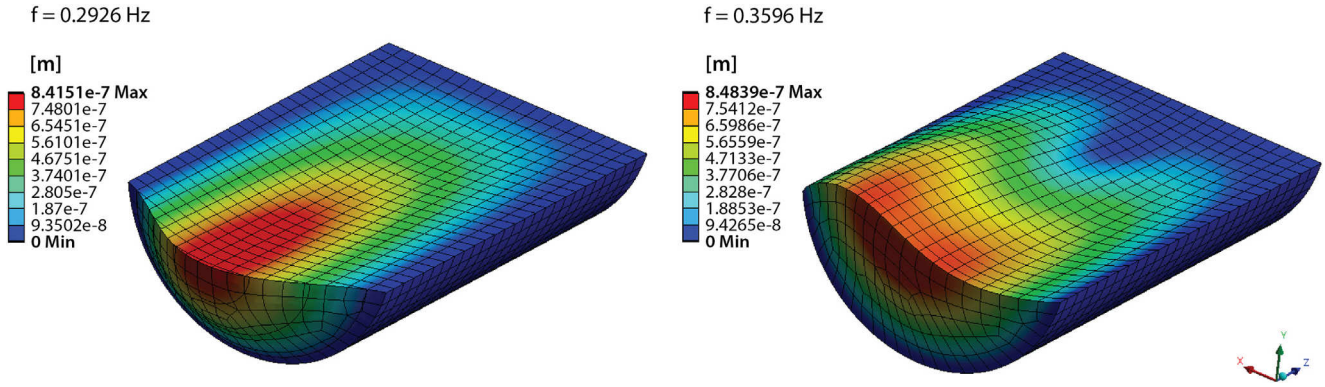

Figure 14. FE model of a valley with aspect ratio equal to 0.6 that reproduces the experimental modes. Illustrated is the fundamental horizontal mode in the direction parallel to the valley axis, with $f_{LONG} = 0.293$ Hz (left) and the fundamental mode transversal to the valley axis, that has both a vertical and a horizontal component, with $f_{TRAN} = 0.360$ Hz (right). As apparent from the colour scale, the deformation affects only the central part of the valley and is approximately zero at the edges as in the experimental data (Fig. 7).

frequency as a function of the seismic bedrock depth at the site, according to eq. (1), when laterally constant *Vs* can be assumed. The 1-D resonance frequency can be converted to depth by using a V_S model or *vice versa*. The detection of 1-D resonances can therefore be used both for seismic site effect assessment and stratigraphic reconstructions.

In case of 1-D resonance, the individual spectra normally show a local minimum in the vertical component and coincident horizontal components with a maximum (or no peaks) at the H/V peak frequency. The minimum in the vertical component is associated to the horizontal polarization of Rayleigh waves, that occurs at the resonance frequency of *SH* waves. The maximum in the horizontal components can both be related to the *SH* wave resonance and to Love waves. Whatever its origin, what matters is that the two horizontal spectra coincide and the minimum in the vertical component is always present.

The other type of resonance is called 2-D and this is the normal resonance of any 2-D object. In this case, the whole object vibrates at the same frequency but:

(1) with different values (f_{TRAN}, f_{LONG}) along its main axes, at least in the general case in which the stiffness and the mass distribution is different around those axes. In particular $f_{TRAN} > f_{LONG}$,

(2) with amplitudes that:

(i) are different for the longitudinal versus the transversal modes. The displacement amplitude along the longitudinal axis is larger than the displacement along the transversal axis, for the same mode number,

(ii) vary along the body axes, as a function of the specific mode shape.

The 2-D resonance is usually easy to distinguish from the 1-D case because it gives two distinct peaks in the horizontal spectral components, the frequencies of which do not vary with space, while their amplitudes do.

The 2-D resonance can be properly acknowledged only by looking at the individual spectral components and not at the H/V curves alone. Two separate longitudinal and transversal horizontal spectral peaks might result in the wider H/V peak described by some authors

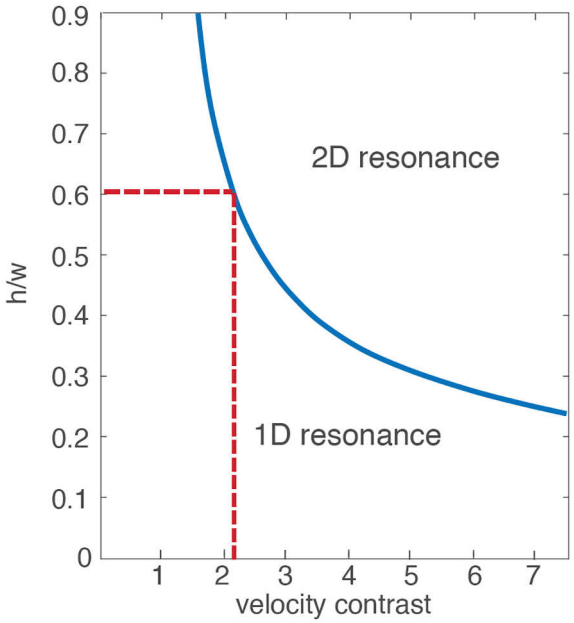

Figure 15. Aspect ratio versus velocity contrast values that should separate 1-D from 2-D resonance, according to Bard & Bouchon (1985).

(e.g. Uebayashi *et al.* 2012). This is an additional reason to analyse the H/V curves always in conjunction with the individual spectra. We recall that the other reasons are the detection of artifactual versus stratigraphic peaks and the recognition of the types of waves contributing to the H/V peaks and troughs.

It is important to note that in order to discern the real longitudinal and transversal frequencies of a resonating body, it is mandatory to record microtremor along the main axes of the geological structures: that is not along the geographical NS and EW direction, as commonly recommended in the H/V guidelines. Failing to do so can completely obscure the results. This is shown in Fig. 13, where the effect of a different instrument orientation on the single spectral components and on the H/V curves is illustrated. Rotating the instrument swaps the longitudinal and transversal spectral peaks and changes the H/V peak amplitude. In the illustrated case, rotating the instrument by 60° makes the two horizontal components coincide perfectly, thus hiding the directional effect. Comparing the frequencies and amplitudes of spectral peaks and spectral ratio peaks of measurements acquired with different instrumental orientations in the 2-D case (and also different from the geological structure main axes) can completely bias any interpretation of the results.

Once the longitudinal and transversal frequencies have been detected, the aspect ratio of the valley section has a positive correlation with the $\frac{f_{\mathrm{LONG}}}{f_{\mathrm{TRAN}}}$ ratio (Fig. 2). The modal sequence $\frac{f_{01}}{f_{00}}, \frac{f_{02}}{f_{00}}, \ldots$ would also have a positive correlation with the aspect ratio (Fig. 3). In addition, the longitudinal-to-vertical peak amplitude pattern across the valley section may be used to infer the shape of the 2-D fundamental modes which reflect the bedrock morphology as observed in Ermert *et al.* (2014). All this information can be used *per se* or can be used to constrain specific finite element models, in the attempt—if needed—of reconstructing geometry of the resonating body, with the caution that errors can be large in case of low frequencies with large experimental uncertainties.

We applied our 1-D versus 2-D classification scheme to the Bolzano basin, which lies at the junction among the branches of three separate valleys, characterized by 1-D-only, 1-D + 2-D and 2-D-only resonance patterns. For the 2-D branches, we found that the $\frac{f_{\mathrm{LONG}}}{f_{\mathrm{TRAN}}}$ method suggested an aspect ratio of 0.6. We generated an Finite Element (FE) model (ANSYS R2 2019) of a sine-shaped valley characterized by an aspect ratio of 0.6 (width 1000 m, maximum depth 600 m), a Young modulus of 3.8 GPa, an equivalent V_S of 600 m s^{-1}, as derived from Fig. 10, average density of the filling material 2000 kg m^{-3} and an average Poisson's ratio of 0.37. The longitudinal size is assumed as infinite and we verified that on intermediate aspect ratio valleys this assumption applies as long as the valley length is at least 3 times the valley width (and this is the case because the valley from Merano to Bolzano is approximately 20 km long). The model was discretized into an 80 m-side mesh and the bottom surface was fixed, in order to simulate a rigid bedrock. The natural frequencies of this model reproduced the observed frequencies with no need of tuning: we found 0.293 Hz as fundamental longitudinal vibration mode and 0.360 Hz as fundamental transversal vibration mode. We observe also that the mode shape is very similar to the experimental findings (compare Fig. 14 with Fig. 7): no motion actually involves the two valley edges for about $\frac{1}{4}$ of the valley width on both sides. Although the model is very basic, it still shows that a valley with that shape, aspect ratio and equivalent *Vs* has resonance frequencies very close to those experimentally observed.

Bard & Bouchon (1985) proposed a relation between the aspect ratio of a valley and the velocity contrast between the filling material and the bedrock that would separate the observation of 1-D from 2-D resonances, which is reported in Fig. 15. According to this relation, the aspect ratio of the studied valley implies a minimum velocity contrast of 2.2 where 2-D resonance is visible. This means that if $V_s \simeq 600$ m s^{-1} for the filling sediments, $V_s > 1300$ m/s^{-1} for the underlying porphyritic bedrock, which is clearly acceptable.

It is interesting to note that this plot has been traditionally used to tell whether 1-D or 2-D effects were expected, starting from a known/supposed aspect ratio. Here, we start from the fact that we know from the experimental data whether we are in presence of 1-D or 2-D effects, we evaluate the aspect ratio from the data themselves and we use the plot to assess the minimum velocity contrast between the sediments and the bedrock, which is relevant information in the seismic site response studies.

Previous authors (Roten *et al.* 2006; Le Roux *et al.* 2012) stated that in order to detect 2-D resonance, simultaneous array measurements across the valley, or reference stations are needed. As a difference compared to these works, we show that the fundamental 2-D resonance features of a geological structure do not necessarily need an array of synchronized instruments to be detected, while an array of synchronized instruments clearly helps in assessing modal shapes.

Also, under the hypothesis of stationary noise, assessing the modal shapes does not require arrays of synchronized instruments: looking at the peak amplitude of the displacement spectra recorded at each site is enough to reconstruct the absolute value of the modal shape (Castellaro & Isani 2019). Assessing the phase requires at least two instruments but this is required only for higher modes (the fundamental mode has the same phase at all sites by definition) and, when several measurements are available, it is rather easy to assess the displacement nodes and infer the phase changes in the deformation acquired even with a single instrument. The most delicate practical aspect in the reconstruction of the mode shapes is the stationarity of the noise level/excitation function. Since in the 2-D case we are normally interested in rather low frequencies, the main ambient noise source below 1 Hz is atmospheric (Gutenberg 1931, 1947, 1958). As far as the recordings are acquired under the

Table 1. Proposal to detect 1-D and 2-D resonances from single-station microtremor acquisitions.

1-D resonance	2-D resonance
Instrumental orientation	
Indifferent	(i) Along the axes of the geological structure (e.g. parallel and perpendicular to a valley axes, parallel to a mountain chain, etc.). (ii) Do NOT follow the geographical NS, EW alignments, unless they coincide with the structural axes of the surveyed geological body. **Failing to do so can have the consequences illustrated in the text.**
Single microtremor measurement	
Spectral features	
Warning. It is given for granted that the user knows how to distinguish peaks of stratigraphic origin from peaks of other origin and that the user knows how to compare the amplitude of recordings acquired at different times (stationarity of the source, see text).	
	Note: placing the instrument at the valley centre or where the maximum depth to bedrock is expected will show the maximum (in amplitude) 2-D effects.
(i) **Always present:** local minimum in the vertical spectral component at the resonance frequency (Rayleigh wave polarization in the horizontal plane). (ii) **Sometimes present:** local maxima in the horizontal spectral components, at the same frequency (Love or *SH* waves).	(i) Local maxima in the two horizontal components, transversal and longitudinal to the valley axis:■ typically at different frequencies ($f_{\text{long}} < f_{\text{tran}}$)■ with different amplitudes ($A_{\text{long}} > A_{\text{tran}}$)
Several (not synchronized) microtremor measurements Along profiles perpendicular to valley axis	
Spatial distribution of the spectral peaks/troughs and of the H/V peak frequencies	
(i) Changes with the depth to bedrock, thus allowing for stratigraphic reconstructions.	(i) Horizontal and H/V peaks remain constant at all sites.
Amplitude of the spectral and H/V peaks	
(i) Depends on the sediment-to-bedrock impedance contrast (and, also as a consequence of this, on the amount of Love waves and on the ellipticity of Rayleigh waves).	(i) The individual spectral amplitudes can be compared in case of stationary sources. The H/V amplitudes can be compared with less restrictions, due to the normalizing capability of the H/V function. (ii) In the displacement spectra, the fundamental longitudinal mode has the maximum amplitude at the valley centre (or where the sediment thickness is maximum). (iii) Allows reconstructing the absolute value (the modulus) of the mode shape.

same weather conditions (preferably in the same day) this condition is normally fulfilled. A second option is to observe the H/V peak amplitude, since the normalization by the vertical component is a rather effective tool, even in case of 2-D resonances, as shown in Fig. 9.

We observed that the displacement induced by the 2-D resonance affects only the central part of the valley and this is observed both from the experimental (Fig. 7) as well as from the modelling point of view (Fig. 14). While the 2-D resonance decays towards the edges, 1-D resonance correlating with bedrock depth may be restored in the valley edges. Alternatively, the edges may show unclear H/V frequency peaks whose correlation with a stratigraphic interface is uncertain. We speculate that the second case may be due to the steepness of the sediment-bedrock interface on the valley edges obscuring or broadening H/V peaks (e.g. Guillier *et al.* 2006).

In conclusion, we underline the importance of assessing the 1-D or 2-D nature of a site experimentally and we propose a workflow scheme to conduct experimental measurements and data analysis in order to assess the 1-D or 2-D resonance nature of a site, by using a single-station approach (Table 1). This is a popular technique used for stratigraphic reconstruction and seismic site effect studies. While the common approach is to look for soil resonances in the H/V ratio only, we note that a careful analysis of the individual spectral components of motion provides important additional information that allows discerning between 1-D and 2-D resonance behaviour. While a complete modal analysis requires multistation synchronized measurements, we suggest that a single-station measurement is sufficient to detect at least the 2-D fundamental resonance frequencies.

This has a strong impact on seismic site response assessment because 2-D resonance is expected to generate large seismic amplification and because this allows to understand when the 1-D assumption does not hold and a 2-D modelling is needed. Concerning stratigraphic reconstructions, in case of 1-D resonances, they are applicable by means of eq. (1), while for 2-D resonances they require additional work (e.g. evaluation of the $\frac{f_{\text{LONG}}}{f_{\text{TRAN}}}$, $\frac{f_{01}}{f_{00}}$, $\frac{f_{02}}{f_{00}}$, ...ratios, modal shape estimation, FE modelling).

ACKNOWLEDGEMENTS

This study was partly funded by the Geological Survey of the Autonomous Province of Bolzano. We thank Giovanni Lattanzi for his support during some field surveys. We thank Volkmar Mair, Corrado Morelli and Maurizio Cucato for providing the stratigraphic and seismic reflection data. We thank Michele Misconel, Martina

Morandi, Giovanni Ronzani and Stephen Slivicki for support for the synchronized measurements. We are grateful to two anonymous reviewers for their constructive comments that helped to improve the manuscript.

REFERENCES

Bard, P.-Y., 1999. Microtremor measurements: a tool for site effect estimation?, in *Proceeding of the Second International Symposium on the Effects of Surface Geology on Seismic Motion, Yokohama, Japan,* 1-3 December 1998, Balkema, Irikura, K. and Joint Working Group on the Effects of Surface Geology and Japanese National Working Group on the Effects of Surface Geology and Association for Earthquake Disaster Prevention, pp. 1251–1279.

Bard, P.-Y. & Bouchon, M., 1980a. The seismic response of sediment-filled valleys. Part I. The case of incident SH waves, *Bull. seism. Soc. Am.,* **70,** 1263–1286.

Bard, P.-Y. & Bouchon, M., 1980b. The seismic response of sediment-filled valleys. Part 2. The case of incident P and SV waves, *Bull. seism. Soc. Am.,* **70**(5), 1921–1941.

Bard, P.-Y. & Bouchon, M., 1985. The two-dimensional resonance of sediment-filled valleys, *Bull. seism. Soc. Am.,* **75,** 519–541.

Bargossi, G.M. *et al.*, 2010. Geological Map of Italy at the scale 1:50.000, Sheet 013 "Merano". ISPRA – Servizio Geologico d'Italia – Provincia autonoma di Bolzano.

Bonnefoy-Claudet, S., Ko¨hler, A., Cornou, C., Wathelet, M. & Bard, P.Y., 2008. Effects of love waves on microtremor H/V ratio. *Bull. seism. Soc. Am.,* **98,** 288–300.

Bour, M., Fouissac, D., Dominique, P. & Martin, C., 1998. On the use of microtremor recordings in seismic Microzonation. *Soil Dyn. Earthq. Eng.,* **17,** 465–474.

Castellaro, S., 2016. The complementarity of H/V and dispersion curves. *Geophysics,* **81,** T323–T338.

Castellaro, S. & Isani, S., 2019. Experimental modal analysis of bridges: how to employ few resources and get it right, *Fast Times,* **24,** 78–83.

Castellaro, S. & Mulargia, F., 2009a. The effect of velocity inversions on H/V, *Pure appl. Geophys.,* **166,** 567–592.

Castellaro, S. & Mulargia, F., 2009b. VS30 estimates using constrained H/V measurements, *Bull. seism. Soc. Am.,* **99,** 761–773.

Castellaro, S. & Mulargia, F., 2010. How far from a building does the ground-motion free-field start? The cases of three famous towers and a modern building, *Bull. seism. Soc. Am.,* **100,** 2080–2094.

Chávez-García, F.J., Raptakis, D., Makra, K. & Pitilakis, K., 2000. Site effects at Euroseistest-II. Results from 2D numerical modelling and comparison with observations, *Soil Dyn. Earthq. Eng.,* **19**(1), 23–39.

Cipta, A., Cummins, P., Irsyam, M. & Hidayati, S., 2018. Basin resonance and seismic hazard in Jakarta, Indonesia, *Geosciences,* **8**(4), 128, doi: 10.3390/geosciences8040128.

Ermert, L., Poggi, V., Burjánek, J. & Fäh, D., 2014. Fundamental and higher two-dimensional resonance modes of an Alpine valley, *Geophys. J. Int,* **198**(2), 795–811.

Fa¨h, D., Kind, F. & Giardini, D., 2001. A theoretical investigation of average H/V ratios, *Geophys. J. Int.,* **145,** 535–549.

Frischknecht, C. & Wagner, J.J., 2004. Seismic soil effect in an embanked deep alpine valley: a numerical investigation of two-dimensional resonance, *Bull. seism. Soc. Am.,* **94**(1), 171–186.

Gosar, A. & Lenart, A., 2010. Mapping the thickness of sediments in the Ljubljana Moor basin (Slovenia) using microtremor, *Bull. Earthq. Eng.,* **8,** 501–518.

Guéguen, P., Cornou, C., Garambois, S. & Banton, J., 2007. On the limitation of the H/V spectral ratio using seismic noise as an exploration tool: application to the Grenoble valley (France), a small apex ratio basin, *Pure appl. Geophys.,* **164**(1), 115–134.

Guillier, B., Cornou, C., Krister, J., Moczo, P., Bonnefoy-Claudet, S., Bard, P.Y. & Fäh, D., 2006. Simulation of seismic ambient vibrations: does the H/V provide quantitative information in 2D-3D structures?, in *Third International Symposium on the Effects of Surface Geology on Seismic Motion, Grenoble, France,* 2006 September 1–August 28, LCPC, Bard, P.Y., Chaljub, E., Cornou, C., Cotton, F., Gueguen, P., 185 pp.

Gutenberg, B., 1931. Microseisms in North America, *Bull. seism. Soc. Am.,* **21,** 1–24.

Gutenberg, B., 1947. Microseisms and weather forecasting, *Meteorology,* **4,** 21–28.

Gutenberg, B., 1958. Two types of microseisms, *J. geophys. Res.,* **63,** 595–597.

Haghshenas, E., Bard, P.Y. & Theodulidis, N., SESAME WP04 Team, 2008. Empirical evaluation of microtremor H/V spectral ratio, *Bull. Earthq. Eng.,* **6,** 75–108.

Ibs-von Seht, M. & Wohlenberg, J., 1999. Microtremor measurements used to map thickness of soft sediments, *Bull. seism. Soc. Am.,* **89,** 250–259.

Lachet, C. & Bard, P.-Y., 1994. Numerical and theoretical investigations on the possibilities and limitations of Nakamuras technique, *J. Phys. Earth,* **42,** 377–397.

Lachet, C., Hatzfeld, D., Bard, P.Y., Theodulidis, N., Papaioannou, C. & Savvaidis, A., 1996. Site effects and microzonation in the city of Thessaloniki (Greece). Comparison of different approaches, *Bull. seism. Soc. Am.,* **86**(6), 1692–1170

Le Roux, O., Cornou, C., Jongmans, D. & Schwartz, S., 2012. 1-D and 2-D resonances in an Alpine valley identified from ambient noise measurements and 3-D modelling, *Geophys. J. Int.,* **191**(2), 579–590.

Lermo, J. & Chávez-García, F.J., 1993. Site effect evaluation using spectral ratios with only one station, *Bull. seism. Soc. Am.,* **83,** 1574–1594.

Lermo, J. & Chávez-García, F.J., 1994. Are microtremors useful in site response evaluation*? Bull. seism. Soc. Am.,* **84,** 1350–1364.

Lunedei, E. & Albarello, D., 2015. Horizontal-to-vertical spectral ratios from a full-wavefield model of ambient vibrations generated by a distribution of spatially correlated surface sources, *Geophys. J. Int.,* **201**(2), 1142–1155.

Malischewsky, P.G. & Scherbaum, F., 2004. Love's formula and H/V-ratio (ellipticity) of Rayleigh waves, *Wave Motion,* **40,** 57–67.

Malischewsky, P.G., Scherbaum, F., Lomnitz, C., Tuan, T.T., Wuttke, F. & Shamir, G., 2008. The domain of existence of prograde Rayleigh-wave particle motion for simple models, *Wave Motion,* **45**(4), 556–564.

Mantovani, A., Valkaniotis, S., Rapti, D. & Caputo, R., 2018. Mapping the Palaeo-Piniada valley, central greece, based on systematic microtremor analyses, *Pure appl. Geophys.,* **175,** 865–881. https://doi.org/10.1007/s00024-017-1731-7

Moczo, P., Labák, P., Kristek, J. & Hron, F., 1996. Amplification and differential motion due to an antiplane 2D resonance in the sediment valleys embedded in a layer over the half-space, *Bull. seism. Soc. Am.,* **86**(5), 1434–1446.

Molnar, S. *et al.*, 2018. Application of microtremor horizontal-to-vertical spectral ratio (MHVSR) analysis for site characterization: state of the art, *Surv. Geophys.,* **39,** 613–631.

Nakamura, Y., 1989. A method for dynamic characteristics estimates of subsurface using microtremor on the ground surface, *Quart. Rep. Railway Tech. Res. Inst.,* **30,** 25–33.

Nakamura, Y., 2000. Clear identification of fundamental idea of Nakamura's technique and its applications, The 12th World Conf. on Earthquake Engineering, Auckland, New Zealand, 30 January–4 February 2000, New Zealand Society for Earthquake Engineering, Paper Number 2656.

Nakamura, Y., 2019. What Is the Nakamura Method? *Seismol. Res. Lett.,* **90**(4), 1437–1443.

Parolai, S., Bormann, P. & Milkereit, C., 2002. New relationship between Vs, thickness of sediments, and resonance frequency calculated by the H/V ratio of seismic noise for the Cologne area (Germany), *Bull. seism. Soc. Am.,* **92,** 2521–2527.

Pöyry, 2017. Deep seismic profile commissioned by the Autonomous Province of Bozen/Bolzano (in German). Technical report, 25 pp.

Roten, D., Fa¨h, D., Cornou, C. & Giardini, D., 2006. Two-dimensional resonances in Alpine valleys identified from ambient vibration wavefields, *Geophys. J. Int.,* **165**(3), 889–905.

Scheib, A., Morris, P., Murdie, R. & Delle Piane, C., 2016. A passive seismic approach to estimating the thickness of sedimentary cover on the Nullarbor Plain, Western Australia, *Aust. J. Earth Sci.,* **63**(5), 583–598.

SESAME Project, 2004. Guidelines for the implementation of the H/V spectral ratio technique on ambient vibrations: measurements, processing and interpretation. SESAME European Research Project WP12, deliverable no. D23.12.

Steimen, S., Fa¨h, D., Kind, F., Schmid, C. & Giardini, D., 2003. Identifying 2D resonance in microtremor wave fields, *Bull. seism. Soc. Am.,* **93**(2), 583–599.

Uebayashi, H., Kawabe, H. & Kamae, K., 2012. Reproduction of microseism HVSR spectral features using a three-dimensional complex topographical model of the sediment-bedrock interface in the Osaka sedimen- tary basin, *Geophys. J. Int.,* **189**(2), 1060–1074.

Van der Baan, M., 2009. The origin of SH-wave resonance frequencies in sedimentary layers, *Geophys. J. Int.,* **178,** 1587–1596.

Zor, E., Özalaybey, S., Karaaslan, A., Tapırdamaz, M.C., Özalaybey, S.Ç., Tarancıoğlu, A. & Erkan, B., 2010. Shear wave velocity structure of the İzmit Bay area (Turkey) estimated from active–passive array surface wave and single-station microtremor methods, *Geophys. J. Int.,* **182**(3), 1603–1618.